

The ionization mechanism of the extended gas in high redshift radio galaxies: shocks or AGN photoionization?

M. Villar-Martín,¹ C. Tadhunter,¹ N. Clark¹

¹ Dept. of Physics, University of Sheffield, Sheffield S3 7RH, UK

Abstract. We have compared the UV line ratios of a sample of very high redshift radio galaxies (HZRG, $z > 1.7$) with shock and active galactic nuclei (AGN) photoionization models, with the goal of determining the balance between jet-induced shocks and AGN illumination in the extended emission line regions (EELR). We find that the UV line ratios cannot be explained in terms of photoionization of solar abundance gas by the classical power law of index $\alpha = -1.5$, which successfully reproduces the general trends defined by the optical line ratios of low redshift radio galaxies. Pure shock models also provide a poor fit to the data. However, photoionization by a power law of index -1.0 provides an excellent fit to the UV line ratios. This suggests that the ionizing continuum spectral shape may depend on radio luminosity and/or redshift, such that it becomes harder as the radio power and/or redshift increase. However, an alternative possibility is that we are seeing the first signs of chemical evolution in these objects, since a power-law of index -1.5 with low metallicity also provides a very good fit to the data.

For the high ionization conditions found in the the HZRG, we show that the power-law photoionization models provide a better fit to the data than the shock models. However, such is the complexity of the shock models that we cannot rule out the possibility that a different combination of input parameters can reproduce the observed spectra.

We further show that the UV line ratios provide a sensitive test of the ionization mechanism for the lower ionization conditions prevalent in some low redshift jet-cloud interaction candidates. For high ionization parameter this discrimination is difficult due to the overlap of shock and power law photoionization models.

1. Introduction

The character of the emission line spectra of powerful radio galaxies is strongly determined by the ionization mechanism of the gas. For most low redshift ($z < 0.1$) radio galaxies photoionization by a central AGN describes rather well the general properties of the optical emission line spectra (*e.g.* Robinson *et al.* 1987). However, when the first high redshift radio galaxies (HZRG, $z > 1.7$) were discovered the situation was not so clear. These objects showed very blue colours and strong Ly α emission — properties expected for galaxies in the process of formation (*e.g.* Spinrad *et al.* 1985, McCarthy *et al.* 1987). It was proposed that some of these HZRG, like 3C326.1, were very young galaxies in which the strong Ly α emission was powered by the young blue stars (McCarthy *et al.* 1987).

However, detailed analysis of the spectra showed that young stars could not explain the general properties of the UV emission lines of HZRG; in particular, the large emission line equivalent widths and the existence of highly ionized species, like CIV and HeII (*e.g.* McCarthy *et al.* 1990).

In the context of the unified schemes for powerful radio galaxies (*e.g.* Barthel 1989), we would expect these galaxies to harbour powerful AGN. This, together with the fact that AGN photoionization succeeded in explaining the optical emission line ratios of low redshift radio galaxies, suggested that the same mechanism dominates the ionization processes in HZRG (McCarthy 1993). In consequence, most attempts to explain the UV emission line spectra of HZRG have invoked pure AGN photoionization.

However, both imaging and spectroscopy of HZRG show that strong interactions are taking place between the advancing radio jet and the ISM of the host galaxy (section 2). Such interactions will generate powerful shocks which will disturb the morphology, kinematics and physical conditions (density, temperature, pressure) of the gas and potentially modify its ionization state. Currently a

Send offprint requests to: M.Villar-Martín, Dept. of Physics, University of Sheffield, Sheffield S3 7RH, UK

key issue in the study of these objects is the relative importance of jet-induced shocks and AGN illumination: do shocks dominate the emission line processes? Or is AGN photoionization dominant with the influence of the shocks mainly manifested in kinematic and morphological disturbances?

We have addressed this problem by studying the UV emission line spectrum of a sample of very HZRG ($z > 1.7$), comparing their line ratios with both shock and AGN photoionization models. We base our study on the UV lines because most of the information we have about HZRG is derived from studies of the UV emission line spectra. At such high redshifts the main optical diagnostic emission lines are shifted into the infrared, and most of the existing IR spectra for the HZRG are of poor quality.

In contrast, at low redshifts we have the opposite problem: the optical diagnostic line ratios are well measured, but the UV spectra are of low quality. For the low redshift objects the optical line ratios have proved inefficient at distinguishing the ionization mechanism unambiguously, although it has been suggested that the UV line ratios might provide a stronger discriminant (Sutherland *et al.* 1993). Therefore, the interest in understanding the emission of the UV lines can be extended to low redshift objects. We propose to develop a diagnostic method to discriminate between shock and AGN ionization in radio galaxies at all redshifts.

We review in section 2 the observational evidence for AGN illumination and shocks in powerful radio galaxies. The data sample is described in section 3 and the diagnostic diagrams in section 4. Sections 5 and 6 present the models and the comparison with the data: section 5 concentrates on the effects of a) varying the shape of the AGN continuum and b) changing the excitation and ionization mechanism (shocks); section 6 analyzes the effects that different physical conditions in the extended gas can produce in the observed UV spectra. In section 7 we extend our diagnostic method to low redshift radio galaxies. Section 8 includes summary and conclusions.

2. Shock vs. AGN photoionization in HZRG ($z > 1$)

2.1. Evidence of AGN illumination in HZRG.

In the popular anisotropic illumination model (*e.g.* Fosbury 1989), it is postulated that quasars hidden in the cores of powerful radio galaxies illuminate the ambient ISM with intense cones of UV/X-ray radiation, with the radiation photoionizing the extended gas within the cones, leading to line emission. This model appears to be consistent with the observed properties of the majority of *low-redshift* radio galaxies. Most importantly, the line ratios measured in the nuclear regions and EELR of radio galaxies, and the trends in these line ratios, generally agree well with photoionization models (Robinson *et al.* 1987; Binette *et al.* 1996). The (weak) alignment of the

EELR with the radio axes (Baum & Heckman 1989) and relatively undisturbed kinematics (Tadhunter *et al.* 1989) are also consistent with anisotropic illumination by the broad radiation cones predicted by the unified schemes. Although there are no radio galaxy EELR which show the clear cone-like morphologies seen in some Seyfert galaxies, this is likely to be due to relatively sparse and inhomogeneous distribution in the early-type host galaxies (Tadhunter 1990).

Anisotropic AGN-photoionization of the ambient ISM is also a viable model for *high-redshift* radio galaxies. The detection of scattered light from a hidden quasar (and also broad line components) in the polarized flux of several HZRG is strong evidence for the existence of luminous quasars which illuminate the ISM (*e.g.* Cimatti *et al.* 1996, Dey *et al.* 1996). Moreover, the presence of large diffuse halos of ionized gas in some HZRG, which extend far beyond the radio structures strongly suggests the existence of a quiescent ISM ionized by the central AGN (*eg.* van Ojik 1995).

McCarthy (1993) constructed a composite radio galaxy spectrum from observations of galaxies with $0.1 < z < 3$. Photoionization calculations reproduce the radio galaxy spectrum rather well and this was presented as an argument in favour of the AGN photoionization as the main ionization mechanism in radio galaxies. However, the composite was built from the spectra of very different objects covering a wide range in redshift, and it is dominated by one or two of the most highly ionized objects. Thus the comparison of this composite spectrum with the models does not resolve the issue of the ionization mechanism for the general population of HZRG.

Villar-Martín *et al.* (hereafter VMBF96) concluded that photoionization by the AGN can explain the positions of a large sample of HZRG in the CIV λ 1550/Ly α vs. CIV λ 1550/CIII] λ 1909 diagnostic diagram. The sequence defined by the data can be parametrized in terms of the so-called ionization parameter, that is, the ratio of the density of ionizing photons impinging on the slab to the density of the outermost gas layer of the slab:

$$U = \frac{1}{cn_H} \int_{\nu_0}^{\infty} \frac{\phi_\nu}{h\nu} d\nu \quad [1]$$

where c is the speed of light, n_H is the density of the gas in the front layer and ν_0 is the Lyman limit frequency. ϕ_ν is the monochromatic ionizing energy flux impinging on the slab. By varying the ionization parameter it is possible to produce the variety observed in the UV line ratios of HZRG. A similar result is obtained at low z : the sequences defined by the optical line ratios of powerful radio galaxies are explained in terms of a sequence defined by U (Robinson *et al.* 1987).

2.2. Evidence of shocks in HZRG.

A possible alternative ionization mechanism in these sources is the ionization by fast shocks produced by violent interactions between the advancing radio jet and the ambient gas: there is already clear evidence for such jet-cloud interactions in HZRG. Firstly, whereas the gas kinematics in most nearby radio galaxies are consistent with gravitational motions (Tadhunter *et al.* 1989; Baum *et al.* 1992), extreme non-gravitational motions are observed along the radio axes in the majority of HZRG (van Ojik 1995; McCarthy *et al.* 1996). Secondly, the extended emission line regions (EELR) are often not only aligned with the radio axis, but closely correlated in detail with the radio emission (Chambers *et al.* 1990; Miley *et al.* 1992; Rigler *et al.* 1992; van Ojik 1995). Even when there are no direct radio/optical associations, the degree of collimation seen in the narrow jet-like EELR along the radio axes of sources like 3C 368 and 3C 324 (Longair *et al.* 1995) is difficult to explain without invoking interactions between the line-emitting gas and the radio jets. The radio-optical asymmetries (McCarthy *et al.* 1991), the relationship between optical structure and radio size (Best *et al.* 1996), and the fact that the extent of the line-emitting gas is almost always smaller than that of the associated radio source (van Ojik 1995), provide further evidence for a close association between the radio plasma and the warm emission line gas.

Recently, we have made a detailed study of the EELR in a sample of low–intermediate redshift radio galaxies which show clear morphological evidence for jet–cloud interactions (Tadhunter *et al.* 1994; Clark & Tadhunter 1996; Clark 1996; Clark *et al.* 1996). This study provides clear evidence that jet-induced shocks determine the distribution, kinematics and physical conditions of the EELR along the radio axes of the objects in the sample. There is also evidence that shocks have an ionizing effect in these sources: in particular, the high temperatures indicated by the the $[\text{OIII}]\lambda 4363/(5007+4959)$ ratio, and the low $\text{HeII}(4686)/\text{H}\beta$ ratio measured in the extended gas, are more consistent with shock-ionization than AGN-photoionization. Even complex multi-phase photoionization models such as those presented recently by Binette *et al.* (1996) and Simpson & Ward (1996) cannot reproduce the measured values of these two line ratios.

With the above discussion in mind, it is imperative that the UV line ratios of HZRG be compared in detail with the predictions of both shock-ionization and AGN-photoionization models.

3. The data

We have constructed a sample which comprises 21 narrow line radio galaxies at high z (most of them have $z > 2$) for which the UV $\text{CIV}\lambda 1550$, $\text{HeII}\lambda 1640$ and $\text{CIII}]\lambda 1909$ emission lines have been measured. We have excluded those objects which show evidence of a BLR. In Table 1, we list

the object names, the line ratios of interest to us here, the redshift and the reference to the observations. Most of the data are taken from the recent thesis by van Ojik (1995) which includes objects selected on the basis of a very steep radio spectrum. The other objects have been selected from the literature with the criteria of having high redshifts, classified as narrow line radio galaxies and with measured fluxes for the three UV lines mentioned above.

The line measurements refer to the integrated emission from the object collected with a long slit aligned with the radio axis. We know that at this redshift, the line luminosities are generally dominated by the extranuclear emission and we can be confident that the general properties of the emitting gas inferred from the spectra describe the extended emitting regions, rather than the emission line regions close to the nuclei.

4. The UV line ratios: the diagnostic diagrams.

We have studied three diagnostic diagrams which involve the $\text{CIV}\lambda 1550$, $\text{CIII}]\lambda 1909$ and $\text{HeII}\lambda 1640$ lines which usually dominate (together with $\text{Ly}\alpha$) the UV spectrum of HZRG. We compare the position in the diagrams of the data with the prediction of pure AGN photoionization and shock models. Shock model calculations for the $\text{Ly}\alpha$ line do not exist in the literature and we have not included this line in our diagrams (see VMBF96 for a detailed study of the $\text{CIV}\lambda 1550/\text{Ly}\alpha$ vs. $\text{CIV}\lambda 1550/\text{CIII}]\lambda 1909$ diagnostic diagram for the same sample of objects studied here and AGN photoionization models).

The data are represented in the diagrams with hollow circles (van Ojik’s data) and solid triangles (other objects). The different models are distinguished by different line types in the diagrams (see Figure captions).

Comparing data and model predictions we want to answer the questions: is it possible to disentangle the main mechanism responsible for the ionization of the gas in HZRG using the UV line ratios? Which models agree better with the data: shocks or AGN photoionization?

5. The influence of the ionizing mechanism on the UV line ratios.

5.1. AGN photoionization models.

We have used the multi-purpose photoionization code MAPPINGS I to build these models. The version described in Binette *et al.* (1993a,b) is well suited for the conditions studied here, since it includes a detailed treatment, not only of the transfer of optically thin lines ($\text{HeII}\lambda 1640$ and $\text{CIII}]\lambda 1909$) but also of the resonant lines, $\text{Ly}\alpha$ and $\text{CIV}\lambda 1550$, which have strongly-geometry dependent emission (VMBF96).

The first step to predict the spectrum emitted by a gaseous region is to define the physical conditions of the gas and the shape of the ionizing continuum. At very high redshift, there are large uncertainties in this respect. The

Table 1. Observed UV line ratios for several high z radio galaxies with no apparent broad component

Name	CIV/CIII]	CIV/HeII	CIII] /HeII	redshift	ref.
Average HZRG	2.05	1.14	0.56		McCarthy 1993
F10214+4724	3.68	1.43	0.39	2.29	Elston <i>et al.</i> 1994
3C294	0.83	1.00	1.20	1.79	McCarthy <i>et al.</i> 1990
3C256-3C239	1.90	1.94	1.05	1.96	Spinrad <i>et al.</i> 1985
0200+015	1.05	1.31	1.25	2.23	van Ojik 1995
0211-122	2.55	1.81	0.71	2.34	"
0214+183	1.67	1.67	1.00	2.13	"
0355-037	1.17	0.73	0.62	2.15	"
0448+091	0.44	0.86	0.86	2.04	"
0529-549	0.22	0.67	3.05	2.58	"
0748+134	1.29	1.20	0.93	2.42	"
0828+193	0.95	1.00	0.95	2.57	"
0943-242	1.70	1.44	0.85	2.92	"
1138-262	0.62	0.62	1.00	2.16	"
1410-001	1.58	1.44	0.92	2.36	"
1558-003	2.25	1.59	0.71	2.53	"
2251-089	2.20	2.54	1.15	1.99	"
4C23.56	3.40	3.92	1.15	2.48	"
4C26.38	3.71	1.56	0.42	2.88	"
4C28.58	0.17	0.19	0.89	2.89	"
4C40.36	1.05	1.11	1.06	2.27	"
4C48.48	2.18	1.65	0.76	2.34	"

optical lines, which have provided a great deal of information about the emitting gas and the ionization processes involved in low redshift radio galaxies, are redshifted into the IR. As mentioned before, the optical (rest-frame) spectra obtained for very high redshift so far are rare. Therefore, it is not possible to use optical line diagnostics to constrain the physical conditions of the emitting gas in our objects.

As a starting point, it is reasonable to assume that these regions are similar to the EELR in low redshift radio galaxies. The discrepancies, if they exist, between the data and the standard models which are successful for the low- z objects will allow us to build more coherent models and therefore, reveal information about the actual conditions of the emitting gas and the nature of the ionizing source. Therefore, the question we will answer in this section is: *can the models which reproduce the optical line ratios of low redshift radio galaxies also explain the UV line ratios of very high redshift radio galaxies?*

Analysis of the optical emission lines has shown that typical densities in EELR apparently photoionized by the central AGN at low redshift are lower than a few hundred. Indeed, if the line emitting gas in the EELR is in pressure equilibrium with the hot phase of the ISM, the EELR densities implied from X-ray observations are of the order or a few particles per cm^{-3} (Clark 1996). McCarthy (1993) reached a similar conclusion using a different approach based on the $\text{Ly}\alpha$ luminosity. Shocks, however, can raise the density up to a few hundred (Clark *et al.* 1996). This increase in the density is not large enough that we need to

worry about the suppression of the emission lines due to collisional deexcitation effects. In our “pure AGN” photoionization model, such an increase in the density will have equivalent effects to a decrease in the flux of the AGN ionizing photons by the same factor. This means that those objects where shocks have compressed the emitting gas – but not ionized it – can be interpreted in terms of a lower ionization parameter (see eq. 1).

We have assumed a density of 10 cm^{-3} at the illuminated face. The behaviour of the gas is isobaric. Therefore, the density at every position in the cloud is adjusted with the temperature to keep the pressure equilibrium. The abundances are assumed to be solar unless another value is specified. The clouds are considered to be radiation bounded (except in section 6.2) and with plane parallel geometry (see VMBF96 for a more detailed description).

5.1.1. Power Law models, $\alpha=-1.5$

We have first investigated whether -1.5 power-law (PL) photoionization models, which are so successful for low- z radio galaxies, are also able to explain the UV line ratios of our sample of high redshift objects. The results are presented in the diagnostic diagrams in Fig. 1. The -1.5 PL sequence is represented on the left diagrams by solid circles connected with a solid line.

A quick look to the left diagrams shows that the -1.5 sequence lies far away from the data points. However, comparing the shape of the model sequence and the trend

defined by the data, the similarity suggests that the data sequence can be explained in terms of the variation in the ionization parameter, as is observed at low redshift.

The influence of geometrical effects

VMBF96 showed that -1.5 PL models can explain the sequence defined by the objects in the Ly α /CIV vs. CIV/CIII] diagnostic diagram when geometrical effects are taken into account. The resonant character of the CIV λ 1550 and Ly α lines makes the escape of the line photons very asymmetric, so that their emission is strongly dependent on the distribution of material inside (and outside, for Ly α) the ionized cones. Provided that the axis of extended emission line nebulosity is not in the plane of the sky, the spectrum we observe is emitted by a mixture of clouds observed from different viewing angles: the clouds further from the observer are seen preferentially from the illuminated face, while the clouds closer to the observer are seen from the rear. In this situation resonant lines are emitted very differently on the two sides of the nucleus; they appear stronger with respect to the other lines on the side which lies further from the observer, and fainter on the other side.

The previous sequences (Fig. 1, left) did not consider the geometrical effects described above: they represent a situation in which geometrical effects due to different orientation angles are cancelled.

In Fig.1 (right) we show the same diagnostic diagrams as before, but geometry is considered. The single PL sequence in the left diagrams has been replaced by two new ones: the long dashed line represents models for clouds observed directly from the illuminated face — this describes the case in which the spectrum of the gas on the far side of the source is dominant — while the dotted line corresponds to the opposite case in which we observe the clouds from the rear (i.e. the clouds on the near side dominate). Any intermediate case is described by a sequence of models intermediate between these.

The back perspective does not help at all to improve the fitting to the data because the resonant CIV line intensity is decreased relative to the other lines. For the “front” sequence, the line ratios involving CIV increase slightly, but not enough to explain the relative faintness of HeII. Moreover, CIII]/HeII is still a problem: geometrical effects do not affect this line ratio and cannot explain its high observed values.

The conclusion is that *photoionization by a power law of index -1.5, which reasonably reproduces the optical line ratios of low redshift radio galaxies cannot explain the observed UV line ratios of HZRG.*

5.1.2. Hot Black Body models

A very hot black body (T \sim 130,000 K) provides an even better fit to the optical line ratios of low redshift radio galaxies than the -1.5 power law usually assumed (Robin-

son *et al.* 1987). We have studied the predictions of these models in the UV spectral range. The results are presented in Fig. 1 (left pannels). Contrary to the conclusion obtained in the optical range, such a continuum *cannot* explain the position of the objects in the UV diagnostic diagrams. The fit is worse than the one produced by the -1.5 PL models — the T \sim 130,000 K black body model falling even further from the data points. The dispersion produced by geometrical effects is similar to the -1.5 PL models. We do not present these models here for simplicity.

Therefore, the models which are successful at explaining the low redshift optical spectra do not work in the UV spectral range for very high redshift objects. An alternative possibility is that the ionizing continuum emitted by the central AGN has a different shape at low and high redshifts. We investigate now the effects that a harder continuum have on the UV line ratios.

5.1.3. A hard ionizing continuum: Power law with index $\alpha=-1.0$

The new models, with a power law of index $\alpha=-1.0$, are shown in the diagnostic diagrams in Fig. 2. As in Fig. 1, the diagrams on the left do not take into account geometrical effects, which, on the contrary, are considered on the right plots. The agreement with the data is excellent. Most of the data points are rather well described by the $\alpha=-1.0$ U-sequence.

The influence of geometrical effects

When considering geometrical effects with the $\alpha=-1.0$ models (Fig. 2, right), most objects lie between the two sequences which represent the back and the front perspective, as expected. For a fixed U we find that, while CIII]/HeII is the same for back and front, the dispersion predicted by the models for different viewing angles is large when line ratios involving CIV are considered and the ionization level of the gas is high. This trend is also suggested by the data: the models seem to envelope a very similar area to the one occupied by the data. Note that the -1.0 PL models can explain the data points in the CIV/Ly α vs CIV/CIII] diagnostic diagram as well as the 1.5PL models.

In summary, *a power law of index $\alpha=-1.0$, where the sequence is defined by the variation of the ionization level of the gas, can explain the observed UV line ratios of HZRG.*

If this result is confirmed, it indicates an evolution of the spectral shape of the ionizing continuum emitted by the central AGN with redshift or luminosity (we are biased to very powerful objects).

There are already some indications of a correlation between the hardness of the AGN continuum and redshift. O’Brien *et al.* (1988) found that quasars of higher redshift show harder UV continua. Francis (1993) concluded that high redshift ($z=2$) AGNs have intrinsically harder mean

continuum slopes ($\Delta\alpha \sim 0.8$) than low redshift AGNs. He also concludes that this is a correlation with redshift and not with absolute magnitude. It is important to mention that these authors study a spectral range longward (in wavelength) of the Lyman limit and, therefore, they do not include the UV ionizing continuum of interest to us in this paper. However, extrapolating their results to shorter wavelengths, the ionizing continuum should also get harder with increasing redshifts.

5.2. The shock models

Another strong possibility to explain the discrepancies between the -1.5 PL (and hot black body) models and the observed UV line ratios is shocks. A high velocity radiative shock can influence the emission line processes through two different mechanisms: a) the generation of a strong local UV photon field in the hot post-shock zone, which can ionize the surrounding medium both upstream and downstream; b) line emission during the radiative cooling of gas behind the hot post-shock zone. We have used the new shock models by Dopita and Sutherland (1995) which take into account both effects. The two main parameters which influence the predicted spectrum are the velocity of the shock and the magnetic parameter defined as $B/n^{1/2}\mu\text{G}\cdot\text{cm}^{-2}$, where B is the pre-shock magnetic transverse field and n is the pre-shock density. Note that we have assumed an ionized helium recombination ratio of $\text{HeII}\lambda 1640/\text{He}\lambda 4686 \sim 7.7$ in order to calculate the $\text{HeII}\lambda 1640$ strength from the $\text{HeII}\lambda 4686$ strengths published in Dopita & Sutherland (1995). Our experience with photoionization models shows that the value of the $\text{HeII}\lambda 1640/\text{He}\lambda 4686$ recombination ratio is insensitive to the physical conditions and the ionization state of the gas.

Shock model sequences are presented in the diagnostic diagrams in Fig. 3. The diagrams on the left show the UV line ratios of the cooling region (post-shock material). The velocity varies between 150 and 500 km s^{-1} and the magnetic parameter between 0 and 4 $\mu\text{G cm}^{-3/2}$. The density adopted is $n(\text{H})=1\text{cm}^{-3}$. The diagrams on the right correspond to the precursor gas emission, that is, material which has not entered the shock but is ionized by its UV photon flux. The velocity is varied (200-500 km s^{-1}) with a fixed magnetic parameter (1 $\mu\text{G cm}^{-3/2}$).

The agreement between the shock and precursor models with the data is very poor. For the range of models which reproduce the observed range of CIV/HeII values, CIII] is too faint, both with respect CIV and HeII, so that the sequences cannot cover the area occupied by the objects. This can be said both for the post-shock and precursor models. Therefore, a mixture will still produce too faint CIII].

Another problem evident from the diagrams is the difficulty of the models at reproducing the sequences defined by the data. In contrast, the trends on the diagnostic dia-

grams are naturally explained in the AGN photoionization context by a sequence in the ionization parameter U .

The conclusion is that *the published shock models cannot explain the observed UV line ratios*. However, shock models are complex and we cannot rule out the possibility that a combination of parameters will be found that reproduces the observed spectra.

6. The influence of the physical properties of the gas.

6.1. The metallicity

So far, we have considered that differences in the ionizing mechanism determine those in the emission line spectra. The physical conditions of the gas can also influence strongly the emission line processes. An interesting and reasonable possibility is that the metallicity of the gas at high redshifts is lower than solar. We have calculated models in which the abundances of the heavy elements are 0.4 times the solar values. The ionizing continuum is the traditional -1.5 PL.

The agreement with the data is excellent as the diagrams in Fig. 4 show. The models are represented by the solid line connected with solid circles. Again, these models can also explain the data points in the CIV/Ly α vs CIV/CIII] diagnostic diagram.

Since the CIV/CIII] line ratio is strongly dependent on U (and not so much on metallicity in 0.4 solar to solar range of values considered) it is interesting to compare the U values required to reproduce the CIV/CIII] line ratio with the values derived for low redshift EELR from the optical line ratios. Most high redshift objects lie in the $\log U$ range [-2,-0.5]. The ionization level of the gas is similar to that observed in highly ionized EELR at low redshift (Robinson *et al.* 1987). However, this is not the trend observed in low redshift jet—cloud interaction objects, where shocks are important (Clark 1996, Clark *et al.* 1996). In these cases the average level of ionization of the gas is lower than that measured for the EELR of radio galaxies where AGN photoionization dominates. If a -1.5 PL is responsible for the ionization of the gas, these results suggest that we are biased towards very powerful objects in which the gas is highly ionized.

If lower metallicities are confirmed at high redshift a harder AGN ionizing continuum is no longer necessary and the classical -1.5 PL is still valid. An interesting consequence is that this would be the first clear evidence for *chemical evolution with redshift* in the host galaxies of powerful radio galaxies.

There is other evidence for chemical evolution with redshift, with decreasing metallicities for younger objects: damped Ly α systems (DLA) at large redshifts ($z \sim 2-3$), which are thought to be produced by protogalactic disks, are measured to have a metallicity $Z \sim 1/10 Z_{\odot}$ (Pettini *et al.* 1994). Although the metallicity evolution revealed

by the DLA might not be valid for all kind of objects, it is suggestive and might also happen in radio galaxies.

6.2. Matter bounded clouds

In spite of the good general agreement between -1.5 PL models and the observed optical line ratios of *low* redshift radio galaxies, there are three problems which the classical photoionization models cannot explain: a) too weak high ionization lines; b) too low electronic temperatures; c) too small range in the ratio $\text{HeII}\lambda 4686/\text{H}\beta$. Several authors have proposed in the past that a contribution of matter bounded clouds could help to solve some of the discrepancies (*e.g.* Viegas & Gruenwald 1988). In a recent paper Binette *et al.* (1996) develop a detailed study around this possibility. They consider two distinct populations of line emitting clouds: a matter bounded component and an ionization bounded component, with the ionization bounded clouds illuminated by the ionizing spectrum escaping from the matter bounded component. A variation in the ratio of the two components can explain the sequences in the optical line ratios on the diagnostic diagrams, and they can also solve the three problems mentioned above.

We have considered these models as a possible solution to the discrepancies between the -1.5 PL models and the data. The authors present the predictions for the $\text{CIV}/\text{CIII}]$, $\text{CIV}/\text{H}\beta$ and $\text{HeII}\lambda 4686/\text{H}\beta$ ratios. Assuming as before, $\text{HeII}\lambda 1640/\text{HeII}\lambda 4686 \sim 7.7$ we can compute the UV line ratios of interest to us.

The models are represented in Fig.4 (short thick solid line). The authors adopt as continuum energy distribution a power law of index -1.3 and select a constant ionizing parameter 0.04. The variable parameter is $A_{I/M}$, which represents the collecting area ratio of the ionization bounded clouds to radiation bounded clouds. The values vary from 0.06 to ~ 4 .

These models are unable to explain the wide range in UV line ratios observed for the high redshift sample. The reason is that the UV line ratios are not so sensitive to $A_{I/M}$ as the optical line ratios, which involve lines produced in partially ionized regions inside the clouds. The UV lines studied here are produced mainly near the illuminated face of the emitting clouds. Unlike at low z , where a simple variation of $A_{I/M}$ can explain the observed trend in the optical line ratios, the UV line ratios of the high redshift sample suggest that changes in U play a more important role.

The harder continuum might be the reason why the models lie closer to the data than the -1.5 PL models (the -1.3 lies between the -1.0 and -1.5 sequences). Adding a matter bounded component to the previous -1.5 PL models will not help to fit the data: CIV/HeII will remain nearly constant and $\text{CIII]}/\text{HeII}$ will decrease slightly (although overlapping in part with the HeII region, CIII] is formed deeper inside the clouds).

Therefore, a mixture of radiation and matter bounded clouds, cannot explain the discrepancies between the -1.5 PL models and the observed data.

6.3. A diagnostic in the optical

Among the possibilities studied here to explain the UV data, low metallicities and a hard power law ionizing continuum produce a good fit to the data. As the models overlap in the UV, a way to discriminate between them is to compare the predicted *optical* (rest frame) line ratios with the observations. One of the few examples of objects with infrared (optical rest-frame) spectroscopy is the radio galaxy 4C40.36 (Iwamuro *et al.* 1996). We have compared the optical line ratios with the values derived from a) the -1.0 power law models and b) the -1.5 power law and 0.4 solar metallicity values, both of which explain the UV line ratios (Table 2). This object is also included in our sample. The UV line ratios ($\text{CIV}/\text{CIII}] = 1.05$, $\text{CIII]}/\text{HeII} = 1.05$ and $\text{CIV}/\text{HeII} = 1.11$) indicate that, for a hard PL of index $\alpha = -1$, the ionizing parameter $U \sim 0.008$ and for the -1.5 PL and low metallicity models, $U \sim 0.002$. The ratios predicted in the optical are given in Tab. 2:

The flux of some of the lines is poorly determined and the errors in the line ratios are large. The most accurate ratio is $\text{OIII}\lambda 5007/\text{OII}\lambda 3727$ whose value is in very good agreement with the -1.0 power law model while the low metallicity model can not account for it. The high values of the ratios $\text{OII}/\text{H}\beta$ and $\text{OIII}/\text{H}\beta$, if confirmed, are also in better agreement with the hard continuum model.

It is clear that optical line ratios are able to discriminate between these two possibilities. The acquisition of good quality optical (rest-frame) spectra of the HZRG will be crucial to test if the models valid for the UV lines can also fit the optical line ratios.

7. Low redshift radio galaxies

In the above discussion we used the UV emission lines as a diagnostic to distinguish between shock and AGN photoionization in the EELR of powerful high redshift radio galaxies.

At *low* redshifts, most of the information we have comes from the optical emission lines. The most recent shock models developed by Dopita and Sutherland (1995, 1996) produce, in general, optical line ratios which overlap with the -1.5 PL predictions. Therefore, the *optical* emission lines do not provide a clear-cut way to distinguish between the mechanisms.

However, the UV line ratios offer a powerful diagnostic for *low* redshift radio galaxies with *low* U values ($\log U \leq -2.0$). For *high* U values, the distinction is difficult, due to the overlap of the shock and -1.5 power law models (see above), and the diagnostics become inefficient at the high ionization end of the diagram. A comparison of Fig. 1 and 3 reveals that the -1.5 power law with $\log U \leq -2.0$

Table 2. Predicted and observed optical line ratios for the radio galaxy 4C40.36 (the models presented are the ones which reproduce the UV line ratios).

	OIII λ 5007/OII λ 3727	OII/H β	NeIII λ 3869/H β	HeII λ 4686/H β	OIII/H β
Observed	3.3 \pm 1.1	5.3 \pm 5.1	4.6 \pm 5.6	1.0 \pm 1.5	17.5 \pm 14.4
Models -1.0 PL ($U=7\times 10^{-3}$)	3.2	5.2	1.2	0.3	16.7
Models low Z ($U \sim 2\times 10^{-3}$)	13.0	1.0	0.9	0.2	13.0

lie far from the shock models, due to the much fainter CIV emission. While these AGN photoionization models produce $\log(CIV/CIII) \leq 0.5$ and $\log(CIV/HeII) \leq 0.2$, the values for the shock models are ≥ 1.0 and ≥ 0.6 and respectively.

As mentioned before, observations of low redshift radio galaxies with strong jet/cloud interactions show that the emitting gas has a low ionization level (Clark & Tadhunter 1996). The spectrum is dominated by the lines emitted by the “cool” high density (i.e. low ionization parameter) gas behind the shock. Therefore, they are suitable for the diagnostics. A good example is the radio galaxy PKS2250-41. Clark et. al (1996) have presented clear evidence of the presence of a jet/cloud interaction in the EELR of this object both from imaging and optical spectroscopy. The optical line ratios indicate that $\log U \sim -3$. Thus the measured UV line ratios have the potential to determine which mechanism dominates the emission line processes in the EELR of this object. The possibility of a -1.0 PL ionizing continuum is rejected because it does not explain the optical line ratios: shock and/or -1.5 PL (or hot black body) are the main possibilities.

8. Summary and conclusions

We have studied the UV line ratios of a sample of *high* redshift radio galaxies to understand which is the main mechanism responsible for the line emission processes.

The models which reproduce the optical line ratios of low redshift EELR (-1.5 power law or hot black body and solar abundances of the gas) cannot explain the UV line ratios of very high redshift radio galaxies. We have investigated several possibilities to explain these discrepancies. The most suggestive one, i.e. shocks produced in jet/cloud interactions, fails to explain the data.

On the contrary, a harder ionizing AGN continuum (power law of index $\alpha=-1$) and the classical -1.5 power law with a low metallicity produce an excellent fit to the data. The first possibility is supported by the existing evidence of an evolution towards harder continuum at higher redshifts of the mean spectral shape of the AGN continuum. The second possibility is supported by the evidence provided by studies of absorption line systems in the line of sight of quasars, which demonstrate abundance of ~ 0.1 solar at very high redshifts.

The UV diagnostic diagrams do not distinguish unambiguously between jet-induced shocks and AGN photoioni-

zation for the HZRG with *high* ionization state because the two sets of models overlap in the diagrams. We note, however, that not only are the sequences on the diagnostic diagrams better explained in terms of photoionization, but the overall ionization state of the HZRG is considerably higher than is measured in well-studied jet—cloud interactions at lower redshifts. Our result do not contradict the existence of shocks in these objects. Rather it suggests that the continuum emitted by the central AGN is the main ionizing source, with the shocks having an important effect on the kinematics and morphology of the gas.

For the lower ionization states, the distinction between the shock and photoionization models is more clear-cut, and the UV diagnostic diagrams are a promising means of distinguishing the major ionization mechanism in the low redshift jet—cloud interaction candidates.

Finally, we note that it is always dangerous to base strong conclusions about the ionization mechanisms on measurements of just a few emission lines in a particular spectral range. Our results are suggestive but not conclusive. It is now essential to check the consistency of the model results by obtaining spectra which cover diagnostics in *both* the optical and UV for individual high and low redshift radio galaxies.

Acknowledgements. We thank Luc Binette for his code MAPPINGS I. M.Villar-Martín thanks Jacco van Loon for useful discussions. M.Villar-Martín acknowledges support from PPARC grant.

References

- Barthel P.D., 1989, ApJ 336, 606
- Baum S., Heckman T., 1989, ApJ 336, 702
- Baum S.A., Heckman T.M., van Breugel W.J.M., 1992, ApJ 389, 208
- Best P.N., Longair M.S., Rottgering H.J.A., 1996, MNRAS 280, L9
- Binette L., Wang J.C.L., Zuo L., Magris C.M., 1993a, AJ 105, 797
- Binette L., Wang J.C.L., Villar-Martín M., Martín P.G., Magris C.M., 1993b, ApJ 414, 535
- Binette L., Wilson A.S., Storchi-Bergman T., 1996, A&A 312, 365
- Cimatti A., Dey A., van Breugel W., Antonucci R., Spinrad H., 1996, ApJ 465, 145
- Chambers K.C., Miley G.K., van Breugel W.J.M., 1990, ApJ 363, 21

- Clark N.E. & Tadhunter C.N. 1996, in *Cygnus A – Study of a Radio Galaxy* (eds. Carilli C.L. & Harris D.E.), CUP, p15
- Clark N.E., 1996, Phd Thesis, University of Sheffield
- Clark N.E., Tadhunter C.N., Morganti R., Killeen N.E.B., Fosbury R.A.E., Hook R.N., Shaw M., 1996, MNRAS in press.
- Dey A., Spinrad H., Dickinson M. 1995, ApJ, 440, 515
- Dey A., Cimatti A., van Breugel W., Antonucci R., Spinrad H., 1996, ApJ 465, 157
- di Serego A.S., Cimatti A., Fosbury R.A.E., Pérez-Fournón I., 1996, MNRAS 279, L57
- Dopita M.A., Sutherland R.S. 1995, ApJ 455, 468
- Dopita M.A., Sutherland R.S. 1996, ApJS 102, 161
- Eales S.A., Rawlings S., Dickinson M., Spinrad H., Hill G.J., Lacy M., 1993, ApJ 404, 578
- Elston R., McCarthy P.J., Eisenhardt P., Dickinson M., Spinrad H., Januzzi B.T., Maloney P., 1994, AJ 107, 910
- Fosbury R.A.E., 1989, in *ESO Workshop in Extranuclear Activity in Galaxies*, eds. E.J.A. Meurs and R.A.E. Fosbury, ESO Scientific Publications, p169
- Francis P.J., 1993, ApJ 407, 519
- Iwamuro F., Oya S., Tsukamoto H., Maihara T., 1996, ApJ 466, 671
- Longair M.S., Best P.N., Rottgering H.J.A. 1995, MNRAS 275, L47
- McCarthy P.J., Spinrad H., Djorgovsky S., Strauss M.A., van Breugel W., Liebert J., 1987, ApJ 319, L39
- McCarthy P.J., Spinrad H., van Breugel W.J.M., Liebert J., Dickinson M., Djorgovski S., Eisenhardt P., 1990, ApJ 365, 487
- McCarthy P.J., van Breugel W.J.M., Kapahi V.K., Vija Y.K., 1991, ApJ 371, 478
- McCarthy P.J., 1993, *Annu. Rev. Astron. & Astrophys.* 31, 639
- McCarthy P.J., Baum S., Spinrad H., 1996, ApJS 106, 281
- Miley G.K., Chambers K.C., van Breugel W.J.M., Macchetto F. 1992, ApJ 401, L69
- Robinson A., Binette L., Fosbury R.A.E., Tadhunter C.N., 1987, MNRAS 227, 97
- O’Brien P.T., Gondhalekar P.M., Wilson R., 1988, MNRAS 233, 601
- van Ojik R. 1995, Ph.D.thesis, Rijksuniversiteit te Leiden
- Pettini M., Smith L.J., Hunstead R.W., King D.L., 1994, ApJ 426, 79
- Rigler M.A., Lilly S.J., Stockton A., Hammer F., Le Fèvre O., 1992, ApJ 385, 61
- Simpson C., Ward M., 1996, MNRAS 281, 509
- Spinrad H., Filippenko A.V., Wyckoff S., Wagner R.M., Stocke J.T., 1985, ApJ 299, L7
- Sutherland R.S., Bicknell G.V., Dopita M.A. 1993, ApJ 414, 510
- Tadhunter C.N., Fosbury R.A.E., Quinn P.J., 1989, MNRAS 240, 225
- Tadhunter C.N., Tsvetanov Z.I., 1989, Nature 341, 422
- Tadhunter C.N. 1990, in *New Windows to the Universe*, eds. F. Sánchez and M. Vázquez, Cambridge University Press, p175
- Tadhunter C.N., Shaw M.A., Clark N.E., Morganti R., 1994, A&A 288, L21
- Tadhunter C., Shaw M., Clark N., Morganti R., 1995, A&A 228, L21
- Viegas S.M., Gruenwald R.B., 1988, ApJ 324, 683
- Villar-Martín M., Binette L., Fosbury R.A.E., 1996, A&A 312, 751.

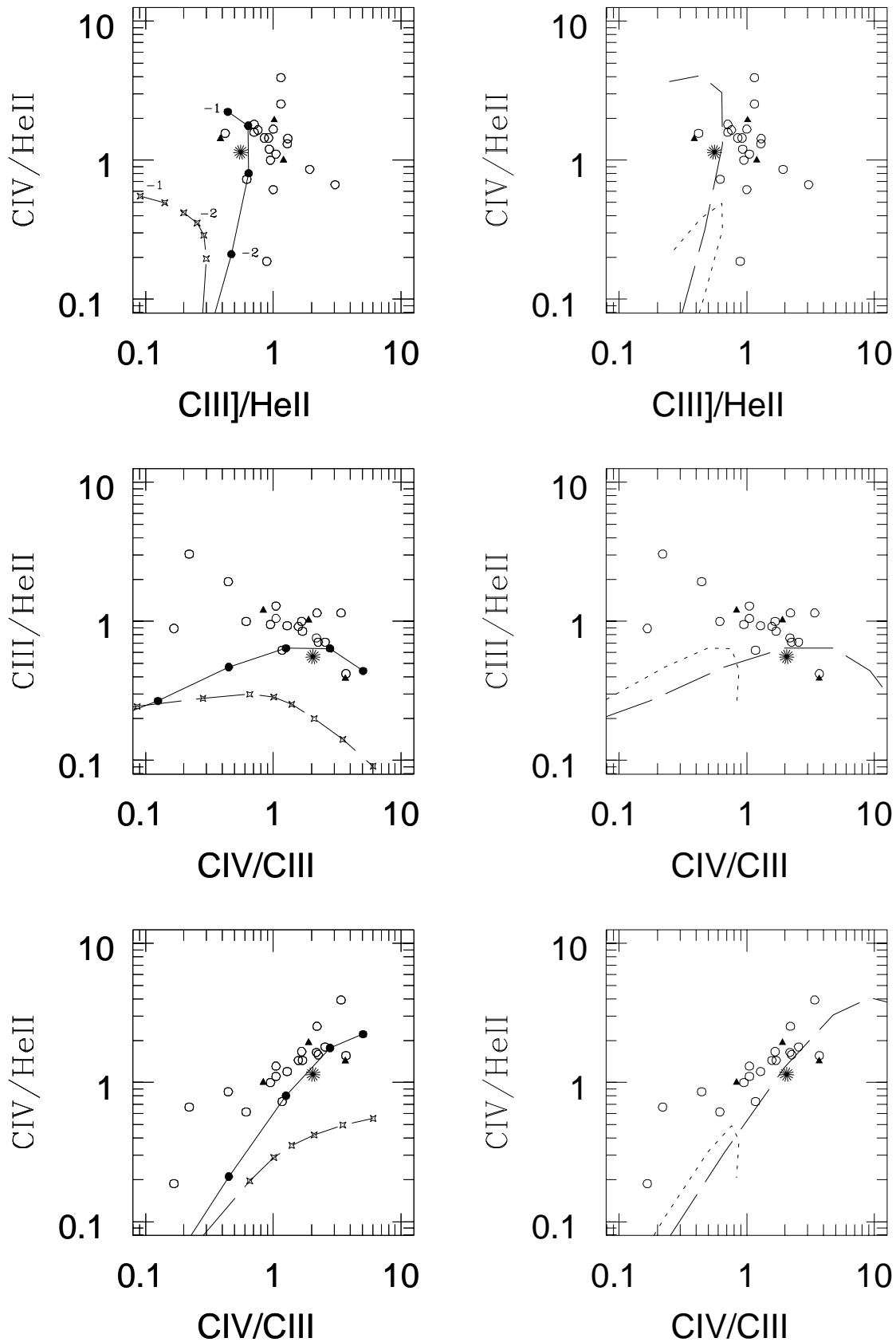


Fig. 1. Left: Comparison of the data sample of HZRG with photoionization models in which the ionizing continuum is: 1) a power law of index -1.5 (solid circles connected by a solid line) 2) Hot black body, $T \sim 130000$ K (stars connected by a long-dash line). The negative numbers indicate $\log U$. Hollow circles are van Ojik's (1995) HZRG and solid triangles other HZRG with published UV line fluxes. The star corresponds to the average HZRG spectrum of McCarthy (1993). **Right:** The two new sequences use a -1.5 power law as ionizing continuum but with geometrical effects considered. The long-dash line describes the spectrum of the clouds seen directly from the illuminated face. The dotted line corresponds to the opposite case, the clouds are observed from the "dark" face. (Model dots have been suppressed for simplicity).

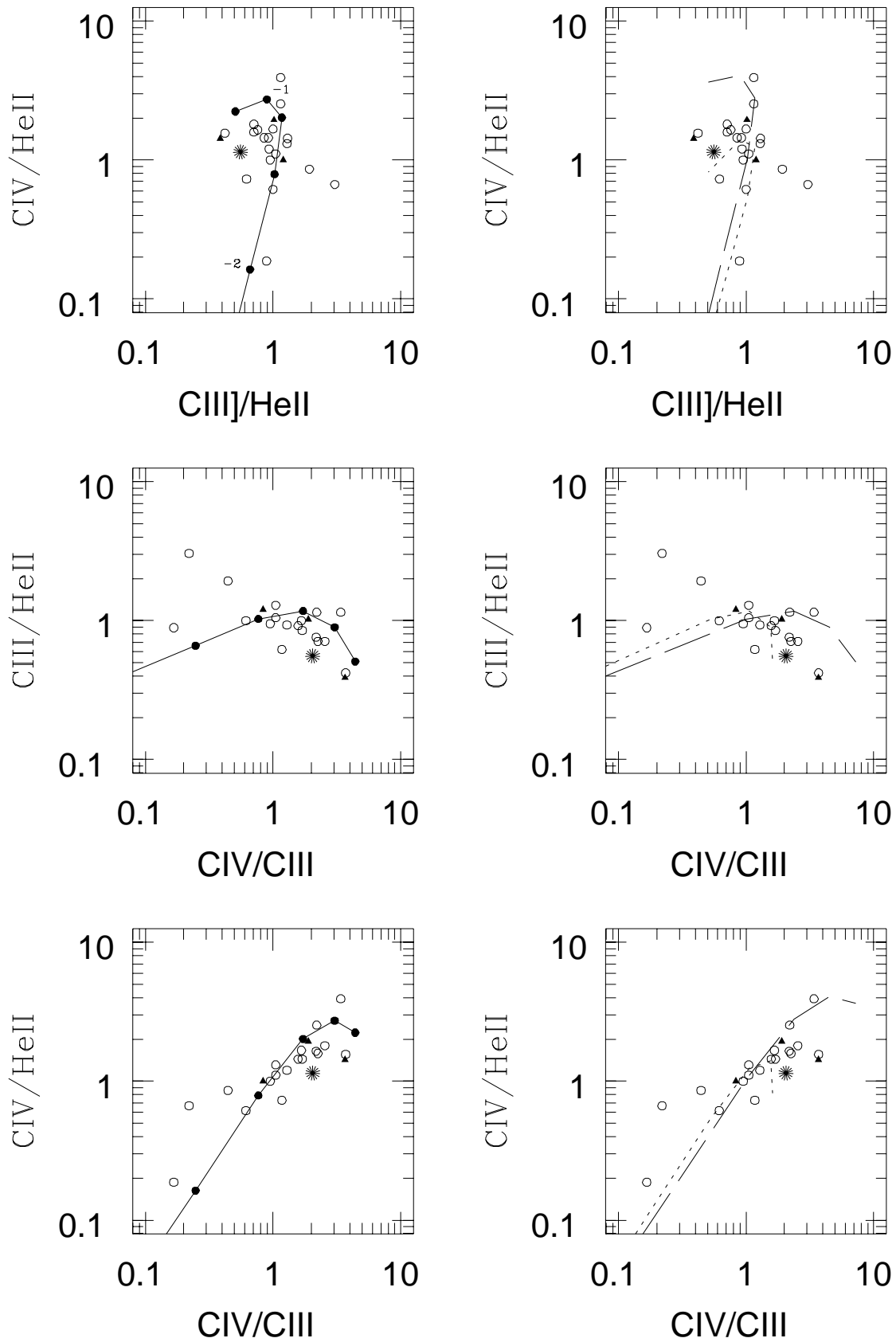


Fig. 2. The ionizing continuum is in the new sequences a power law of index $\alpha = -1.0$ (symbols as in Fig. 1). The improvement to fit the observed positions is remarkable.

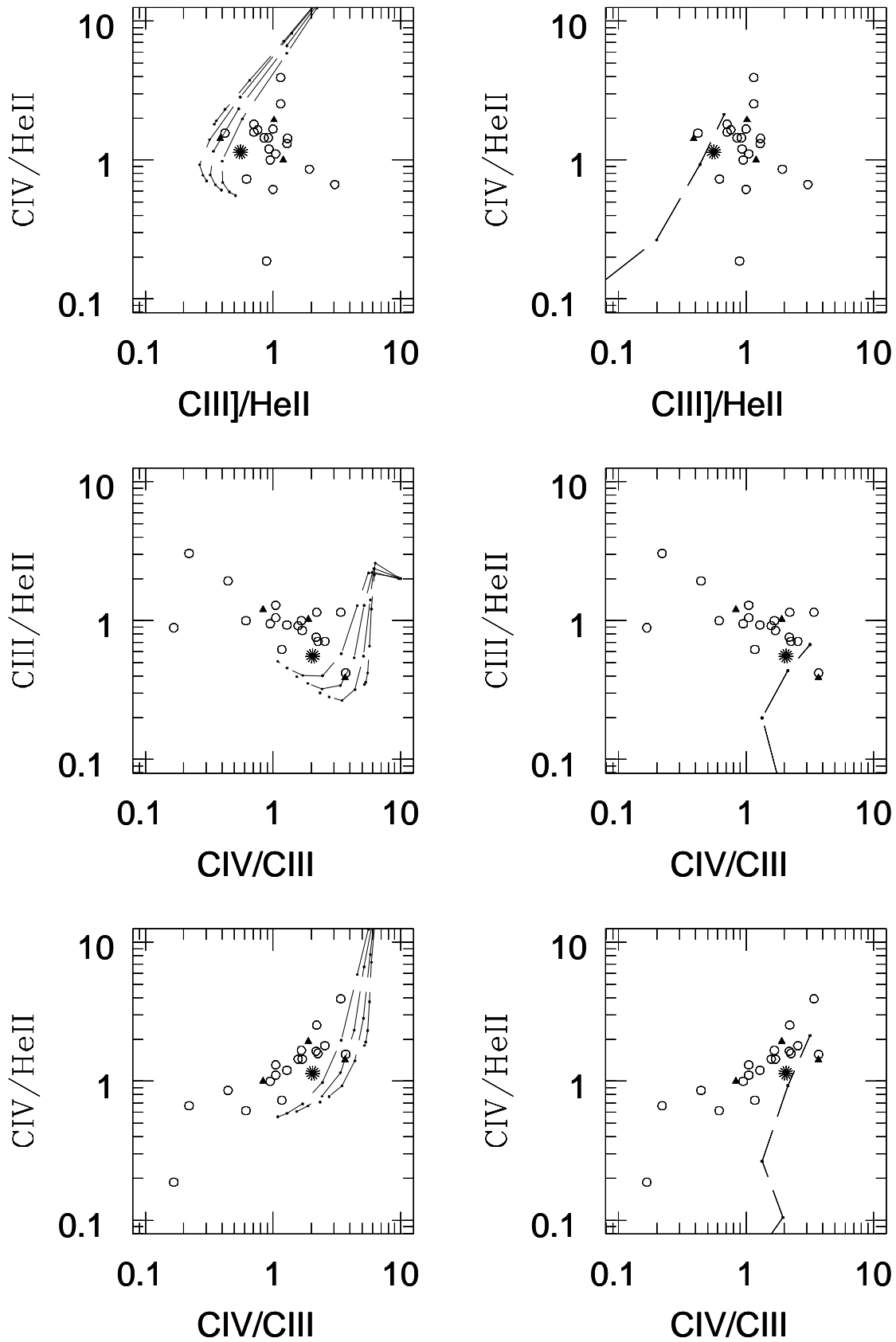


Fig. 3. Comparison of the data sample of HZRG with the new shock models by Dopita & Sutherland (1995): the diagrams on the left show the UV line ratios predicted for the cooling radiation lines. The diagrams on the right present the models for the precursor gas, ionized by the upstream photons emitted by the shock. These shock models are unable to explain the observed line ratios. For the cooling radiation models, both velocity ($150\text{-}500\text{ km s}^{-1}$) and magnetic parameter ($0\text{-}4\ \mu\text{G cm}^{-3/2}$) change, while for the precursor the velocity is varied ($200\text{-}500\text{ km s}^{-1}$) with a fixed magnetic parameter ($1\ \mu\text{G cm}^{-3/2}$).

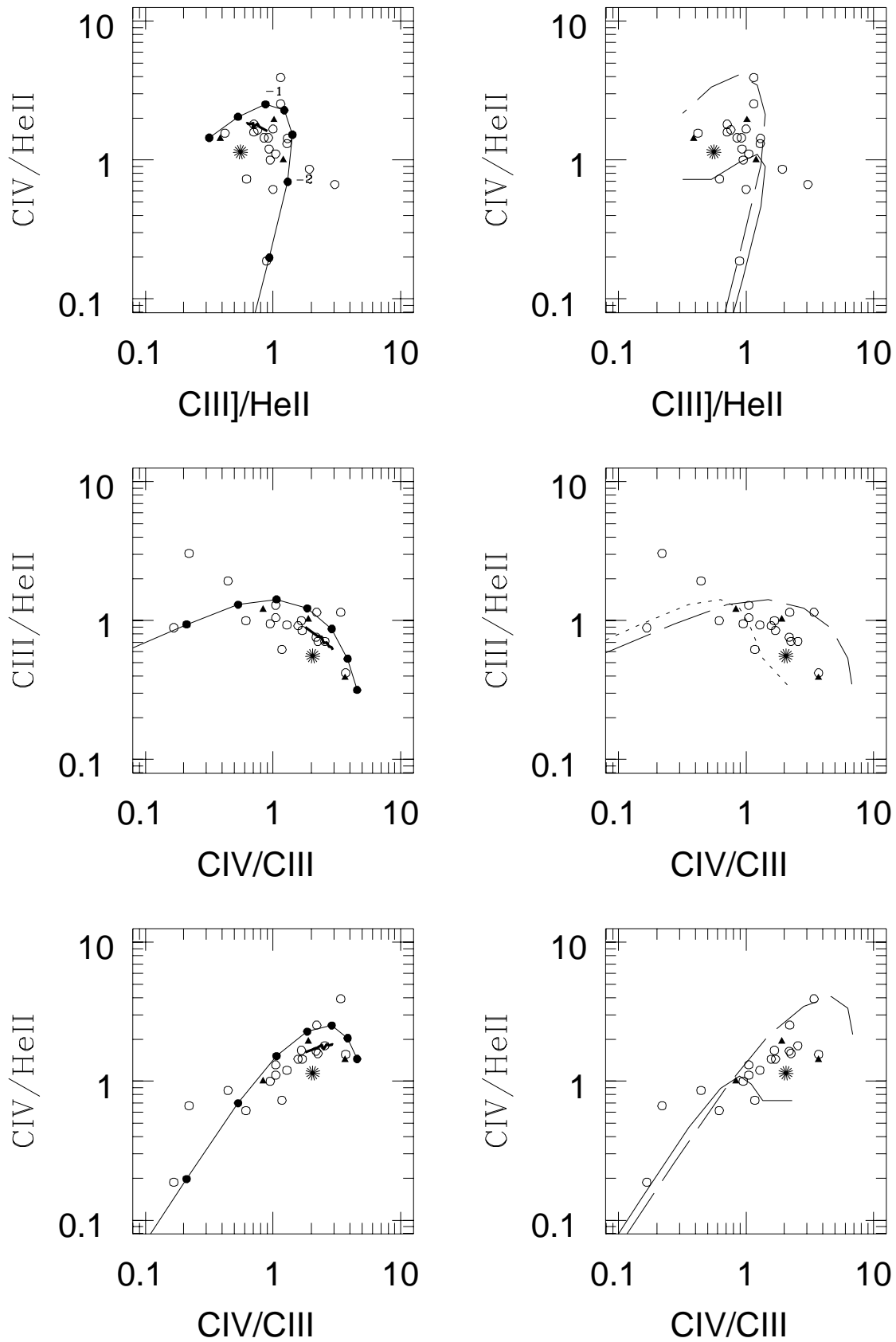


Fig. 4. The ionizing continuum is in the new sequences a power law of index $\alpha = -1.5$ (symbols as in Fig. 1). In this case the abundance of the heavy elements are decreased by a factor of 0.4 with respect the solar values. The agreement between the models and the data is excellent. The thick short solid line corresponds to the sequence of models proposed by Binette et al. (1996) with a mixture of matter bounded and radiation bounded clouds.